The Eighteenth International Symposium on Artificial Life and Robotics 2013 (AROB 18th '13),
Daejeon Convention Center, Daejeon, Korea, January 30-February 1, 2013

Estimating a floodwater from MODIS time series and SRTM DEM data

Youngjoo Kwak[1], Jonggeol Park[2], and Kazuhiko Fukami[1]

[1]International Center for Water Hazard and Risk Management, Tsukuba 305-8516, Japan
[2] Tokyo University of Information Sciences, Chiba 265-8501, Japan
(Tel: 81-29-879-6779, Fax: 81-29-879-6709)

[1]kwak55@pwri.go.jp

Abstract: Extreme climate event, such as heavy rainfall and Typhoon, is anticipated to escalate extreme floods. In fact, many flood plains in the Asian-Pacific region have already experienced a rising number of flood disasters. In this circumstance, real-time flood mapping with automatic detection technique is increasingly important in emergency response efforts. However, current mapping technology is still limited in accurately expressing information in flood areas such as inundation depth and extent. For this reason, the authors attempt to improve a floodwater detection method with a simple algorithm for a better discrimination capacity to discern flood areas from turbid floodwater, mixed vegetation areas, snow, and cloud. In this research, pixel classification was performed on the Moderate Resolution Imaging Spectroradiometer (MODIS) time series images (8-day composites, MOD09A1, 500-m resolution) for floodwater detection. The purpose of this image classification was to estimate a flood area based on the spatial distribution of a nation-wide flood from near real-time MODIS images coupled with a digital elevation model (DEM). Moreover, the authors improved the accuracy of the water extent boundary using a 8-direction tracking algorithm to find the same level between flood-prone area and non-flood area. The results showed the superiority of the developed method in providing instant and accurate flood mapping by using three algorithms, which indicates decision tree, modified land surface water index (MLSWI) and 8-direction tracking based on DEM data.

Keywords: Flood mapping, floodwater, MODIS, DEM.

1 INTRODUCTION

Over the last decades, the number of fatalities and the scale of economic damage caused by river floods have considerably increased worldwide. Moreover, extreme rainfall and typhoon are projected to increase the frequency and magnitude of river floods in the future, which are likely to cause a further increase in flood risk leading to more human and economic damage given the current population growth and the ongoing accumulation of value assets in river deltas. The Asia-Pacific region is particularly vulnerable to the impacts of natural disasters [13]. Satellite remote sensing is a useful tool for interpretation and analyses of water bodies, including floodwater with cost-effective, accurate monitoring at frequent time steps over large areas. Various remote sensing methods have been introduced to detect surface water or estimate floodwater during flooding while considering floodplain topography [4, 7, 9, 12]. Flood detection is one of the classical themes of satellite-based remote sensing. Despite its usefulness, satellite-based remote sensing has also limitations, particularly, in spatial coverage and detection of mixed floodwater. Gao [3] developed the Normalized Difference Water Index (NDWI), a satellite-derived index from near-infrared (NIR, band 2) and short wave infrared (SWIR, band 6) bands: $NDWI=(\rho_{0.85}-\rho_{1.24})/(\rho_{0.85}+\rho_{1.24})$, where ρ represents the radiance in reflectance units. Both $\rho_{0.85}$ and $\rho_{1.24}$ are the reflectance at 0.85 μm and 1.24 μm wavelength, respectively. NDWI is used to derive water fraction and a flood map from MODIS data. Xiao et al. [14, 15] used the multi-temporal MODIS images (8-day composites, MOD09A1, 500-m resolution) to extend the approach to larger regions, south China, South and Southeast Asia. They used a relaxed set of criteria, LSWI+0.05 > EVI or LSWI+0.05 > NDVI, to identify flooded paddy rice fields. The land surface water index (LSWI) is calculated using the spectral signals in shortwave infrared (SWIR) and in NIR ranges to detect water at the soil surface [4].

The purpose of this study was to detect flood areas in near real-time accurately and rapidly, based on the spatial distribution of nationwide flooding by using an improved version of MODIS indices so that mapping the spatial and temporal dynamics of flooding is possible. To determine the water extent boundary more accurately, the authors improve an extraction method of surface water with a simplified decision tree method using reflectance of MODIS bands 6 (CH6) and 7 (CH7) acquired from a regional flooding. The improved method was then applied to the Indus River basin in Pakistan, which was selected as the prime research focus area. The selected area suffered from a huge, severe flood caused by abnormally heavy rainfall from late July to early August 2010.

2 DATA

2.1 MODIS MYD09A1

The Moderated Resolution Imaging Spectroradiometer (MODIS) is an Earth Observing System (EOS) instrument onboard the Terra and Aqua platforms, launched in December 1999 and May 2002, respectively. The sensor scans ±55° from nadir in 36 spectral bands. During each scan, 10 along-track detectors per spectral band simultaneously sample the earth. From its polar orbit, MODIS provides day-time and night-time global coverage every 1 to 2 days [8]. MODIS Surface Reflectance products are the estimates of surface spectral reflectance as if they were measured at the ground level in the absence of atmospheric scattering or absorption. The MODIS L3 8-day composite surface reflectance product (MYD09A1) provides reflectance values for bands 1-7 from the MODIS Level 1B land bands, which are centered at 0.648 μm, 0.858 μm, 0.470 μm, 0.555 μm, 1.24 μm, 1.64 μm, and 2.13 μm at 500-meter resolution in a gridded level-3 product in the sinusoidal projection [10].

2.2 SRTM DEM

The Shuttle Radar Topography Mission (SRTM) obtained elevation data on a near-global scale to generate the most complete high-resolution digital topographic database model of the Earth. SRTM consisted of a specially modified radar system that flew onboard the Space Shuttle Endeavour during an 11-day mission in February of 2000. It used dual radar antennas to acquire interferometric radar data, processed to digital topographic data at 1 arc-sec resolution. SRTM is an international project spearheaded by the National Geospatial-Intelligence Agency (NGA) and the National Aeronautics and Space Administration (NASA) [2]. The elevation layers, DEM, are based on a combination of the original SRTM-3 and DTED-1 elevation models of SRTM. The DEM is provided in geographic projection (latitude/longitude) referenced to the WGS84 horizontal datum and EGM96 vertical datum. The DEM were acquired from Hydrological data and maps based on the SHuttle Elevation Derivatives at multiple Scale (HydroSHEDS) [6, 11]. In this study, DEM is used to calculate potential flood areas at 15 arc-second resolution (approximately 500 meters at the equator).

3 METHODOLOGY

The proposed three-step process reduces errors in the direct extraction of water bodies including floodwater. First step is a decision tree method. Second step is the new flood index, Modified LSWI (MLSWI). Third step is a 8-direction tracking algorithm based on DEM, which uses the flow direction of the same elevation pixels resulting from the previous two steps.

3.1 Decision tree method

Illustrations Decision tree classification is employed on 500 m MODIS reflectance images, in which regions of interest as samples are collected from each flood case for trial, to generate the map by using a post-classification water detection process while comparing with SRTM Water Body Data (SWBD) product. Decision tree classification can be divided into two categories: water surface and dry land surface. Water surface areas are considered to be permanent water bodies such as rivers, lakes, and ponds while dry land areas are considered to be non-water areas that are never flooded. A water surface needs to satisfy the following three conditions to be extracted as water areas: band 7 (CH7) < 10%, band 1 (CH1) +10% > band 2 (CH2) and band 3 (CH3) < 20% (e.g., forest = 0.14, clean water = 0.1, Fig. 1.A). The reflectance of bands 6 and 7 are lower than the other bands in the case of surface water such as clean water, muddy water, and floodwater, which reflect the temporal-spatial pattern of water content (Fig. 1.B).

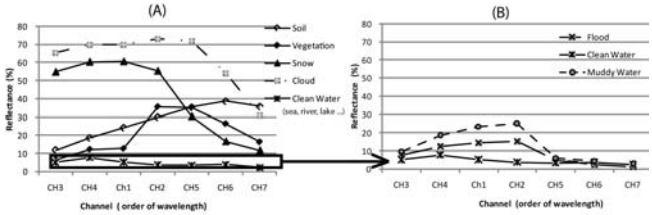

Fig. 1. Spectral reflectance of the land cover classification (A) and the characteristic of the turbid water in flooding (B)

3.2. Modified LSWI

After examining the water and land pixels using the decision tree classification, the flood map is produced based on the modified LSWI (MLSWI) by comparing it with NDVI, NDWI and LSWI, which are the most frequently used and has been proved effective in detecting soil moisture, vegetation and water-related objects, though their detecting ability is somewhat different depending on their characteristics [1, 5]. These indices are calculated as follows:

$$NDVI = \frac{R_{RED} - R_{NIR}}{R_{RED} + R_{NIR}} \quad (1)$$

$$NDWI = \frac{R_{RED} - R_{SWIR}}{R_{RED} + R_{SWIR}} \quad (2)$$

$$LSWI = \frac{R_{NIR} - R_{SWIR}}{R_{NIR} + R_{SWIR}} \quad (3)$$

where, R_{RED}, R_{NIR}, and R_{SWIRD} are reflectance values of MODIS bands 1, 2 and 7.

Compared with the extraction of the floodwater, MLSWI was modified and proposed as a new algorithm for identifying flood areas by using the combination of NIR (841-875 nm, band 2) with SWIR (1 628-1 652 nm, band 7). Equation (4) for MLSWI used in this study is as follows:

$$MLSWI_{Flood} = \frac{1 - R_{NIR} - R_{SWIR}}{1 - R_{NIR} + R_{SWIR}} \quad (4)$$

3.3. Tracking algorithm

After determining floodwater from MLSWI, tracking algorithm for calculating the floodwater boundary is applied to each pixel as the height difference between floodwater area and non-flood area. The floodwater flows into the next pixel with the lower DEM among 8-direction pixels (Fig. 2.). The relative height of floodwater pixel (Floodwater_DEM) indicates the potential flood inundation depth of a given target pixel with the accuracy of 1 m. In the case of Floodwater_DEM ≧ Non-flood_DEM, Fig. 2 shows that floodwater area is calculated because it means that flooding is expected to occur over such pixels.

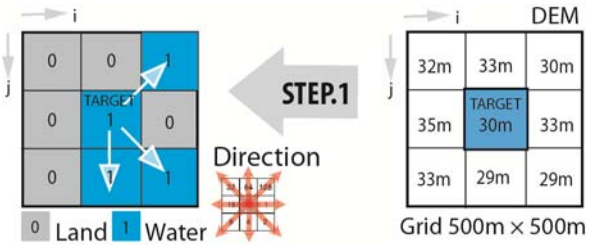

Fig. 2. Flood map from the MLSWI and DEM algorithm in the Indus river flood case

4 RESULT

This study focused on the characterization of flood index for the flood mapping by using a comprehensive approach within a whole basin, solely based on remotely sensed data sources via open internet. The pixel-based water detection for flood identification using training data, and the application in flood area was obtained according to the simple index model process with spectral influences between land cover types water and land. As a result, the MLSWI threshold, the critical value of the reflectance ratio was found at 0.5 for detecting water bodies, such as clean water, muddy water, and turbid floodwater. On the other hand, NDVI, NDWI and LSWI, which usually detect water bodies at a critical reflectance ratio of over 0.5, fail to distinguish water from dry land in some cases, especially when the area contains snow or cloud cover. The process of integrated floodwater detection was made possible to estimate the water extent boundary using a 8-direction tracking algorithm to find the same level between floodwater area and non-flood area, because we found particularly an underestimation of floodwater pixels obtained from MLSWI. Fig. 3 showed the superiority of the developed method in providing instant and accurate mapping of not only water extent but also indirect flood detection for a 2010 extreme event. Flood map was generated with 500 m resolution product in Fig. 3.b. On the other hand, the permanent water body was marked in Fig. 3.d. Moreover, the satellite-derived product uncertainties in the Indus river basin were verified through ground gauge stations by examining actual high water marks and ALOS PALSAR images.

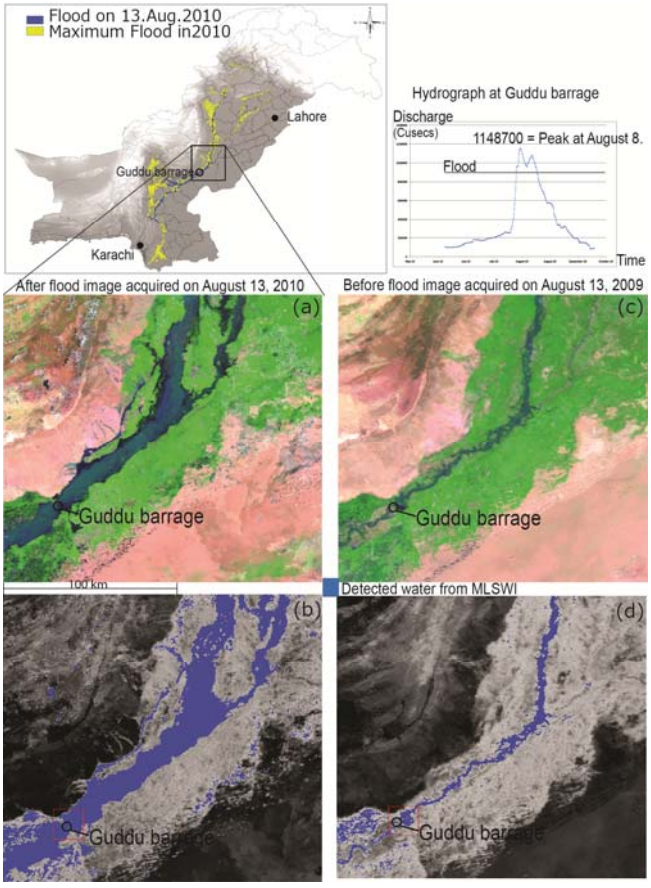

Fig. 3. Flood map from the MLSWI and DEM algorithm in the Indus river flood case

5 CONCLUSION

To conclude, the authors suggested to consider the spatial resolution in horizontal and vertical directions for detecting floodwater. We improved the accuracy of detecting flood areas in the Indus River basin from near-real-time MODIS images of 500 m resolution by using a MLSWI and DEM tracking algorithm. Particularly MODIS images have a higher practicability to detect water body because of moderate-resolution optical sensor (250-500 m) and high temporal resolution (daily). It is clear that MLSWI is detecting directly floodwater during the period of flooding to reduce the ambiguity of floodwater. And DEM surface has the effect of the buffer zone at the boundary of the flood extent which is typically 1 meter vertical resolution in turbid floodwater and mixed vegetation areas. Ultimately, this new approach for nationwide flood map in this study is expected to play an important role to support emergency relief efforts in high-risk flood areas not only in a national level but also Asia-Pacific region.

However, this approach has a limited evaluation of a real flood differed from a hydrological inundation simulation. In addition, MODIS image is easily affected by weather conditions, especially by cloud cover. Also a pixel of 500 meter is too coarse to estimate the temporal dynamics of flooding at different pixels, the authors are planning to improve the spatial resolution in horizontal and vertical directions by using the integrated high resolution images and self-organizing map (SOM) neural network for detection of floodwater area on the land surface. Moreover, the combination of SAR and ASTER image should be further considered to improve the accuracy of flood detection.

ACKNOWLEDGEMENTS

This research was supported by the Ministry of Education, Culture, Sports, Science, and Technology (MEXT)/Japan Society for the Promotion of Science (JSPS) KAKENHI Grant-in-Aid for Young Scientists (B: 24710211).

REFERENCES

[1] Ceccato, P., Flasse, S., Tarantola, S., Jacquemond, S., and Gregoire, J.M. (2001), Detecting vegetation water content using reflectance in the optical domain. Remote Sensing of Environment 77:22–33

[2] Farr T., P. Rosen, E. Caro, R. Crippen, R. Duren, S. Hensley, M. Kobrick, M. Paller, E. Rodriguez, L. Roth, D. Seal, S. Shaffer, J. Shimada, J. Umland, M. Werner, M. Oskin, D. Burbank, Alsdorf D. (2007), The Shuttle Radar Topography Mission, Review of Geophysics 45

[3] Gao, bo-cai (1996), NDWI a normalized difference water index for remote Sensing of Vegetation Liquid water from space, Remote Sensing of Environment 58:257-266

[4] Islam A.S., Bala. S.K. and Haque. M.A. (2010), Flood inundation map of Bangladesh using MODIS time-series image, J. Flood Risk Management 99(4):333–339

[5] Kwak Y, J. Park, A. Yorozuya, K. Fukami, (2012), Estimation of flood volume in Chao Phraya river basin, Thailand from MODIS images coupled with flood Inundation level", IEEE-IGARSS2012, pp887-890

[6] Lehner B., K, Verdin, Jarvis A. (2006), HydroSHEDS Technical Documentation, Version 1.0, World Wildlife Fund US, Washington DC, pp. 1-27

[7] Ordoyne C., Friedl M.A. (2008), Using MODIS data to characterize seasonal inundation patterns in the Florida Everglades, Remote Sensing of Environment 112:4107-4119

[8] Pinheiro A.C.T., Descloitres J., Privette J.L., Susskind J., Iredell L., Schmaltz J. (2007), Near-real time retrievals of land surface temperature within the MODIS Rapid Response System, Remote Sensing of Environment 106:326–336

[9] Sakamoto T., Nguyen V., Kotera A., Ohno H., Ishitsuka N., Yokozawa M. (2007), Detecting temporal changes in the extent of annual flooding within the Cambodia and the Vietnamese Mekong Delta from MODIS time-series imagery, Remote Sensing of Environment 109 (3):295–313

[10] USGS, The United States Geological Survey, last access:
Jan.2011,https://lpdaac.usgs.gov/lpdaac/products/modis_products_table/surface_reflectance/8_day_l3_global_500m/myd09a1

[11] USGS, HydroSHEDS, Technical Documentation Version 1.0 1-27, 2006, http://hydrosheds.cr.usgs.gov/

[12] Weng Q., Hu X., Liu H. (2009), Estimating impervious surfaces using linear spectral mixture analysis with multi-temporal ASTER images, International Journal of Remote Sensing 30:4807–4830

[13] World Bank (2005), Natural Disaster Hotspots: Case Studies, Disaster Risk Management Series, ISBN 0-8213-6332-8 pp.1-184

[14] Xiao X., Boles S., Frolking S., Li C., Bau J.Y. Salas W. (2006), Mapping paddy rice agriculture in South and Southeast Asia using multitemporal MODIS images. Remote Sens Environ 100:95–113

[15] Xiao X., Boles S., Liu J., Zuang D., Frolking S. Li C. (2005), Mapping paddy rice agriculture in southern China using multitemporal MODIS images. Remote Sensing of Environment 95:480–492